UNIVERSITY OF TOULON

December 22, 2023

Modeling and Control of Underwater Vehicle: SPARUS

By:

Abubakar Aliyu BADAWI

N^o **étudiant: 022303696**

Contents

List of Figures

List of Tables

1 Introduction

The Sparus AUV is a high-tech underwater vehicle with advanced features for exploring and researching underwater areas. In this project, I'm closely studying how the Sparus AUV moves in the water, focusing on figuring out things like its added mass and drag. By carefully creating models and using simulations, I hope to understand better how the Sparus AUV behaves underwater and what it can do.

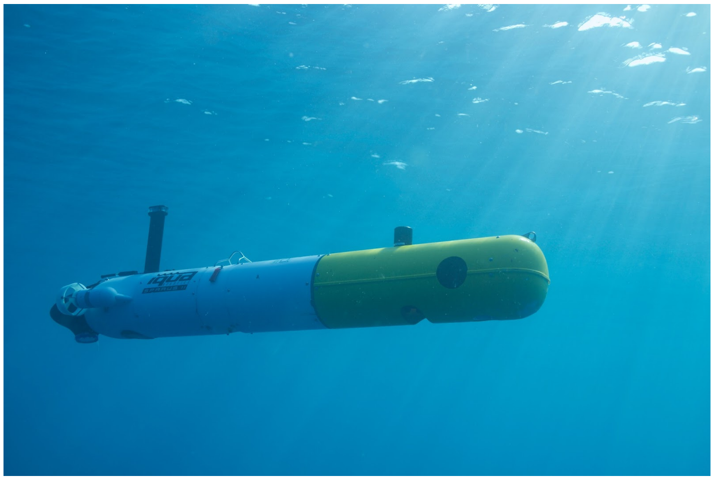

Figure 1: The Sparus AUV

1.1 Aim

To gain in depth understanding of underwater robotics through the modeling and control of the Sparus Autonomous Underwater Vehicle (AUV).

1.2 Objectives

This project aims to formulate the parameters essential for characterizing the dynamic equations of the Sparus Autonomous Underwater Vehicle (AUV). Furthermore, I will validate these parameters through simulations in MATLAB. This foundational exploration seeks to enhance my understanding of the Sparus AUV's dynamic behavior through the steps below:

1. Analyzing the magnitude and order of the global real mass matrix of the Sparus AUV
2. Computing the added mass matrix and the buoyancy center of the Sparus and comparing it to that of the gravity center.
3. Comparing the added mass matrix of the main solid with other bodies and conclude.
4. Estimation of all drag matrices.
5. Complete and validate the simulator.
6. Investigating the impact of the different coefficients in the global mass matrix.
7. Investigating the impact of the drag forces of the different bodies

2 Coordinate Frame Definition for the Sparus AUV

The Sparus has its origin frame, denoted as (F_b) established at the system's midpoint. In this frame, the x-axis of F_b is positioned between the two thrusters, pointing towards the hemisphere section of the Sparus, while the z-axis extends towards the opposite side of the antenna, as illustrated in Figure below.

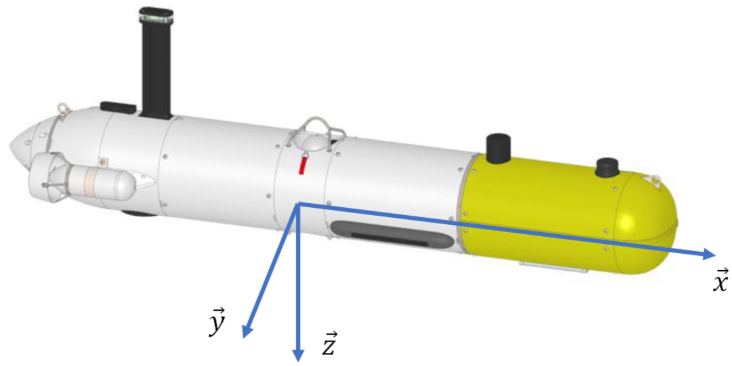

Figure 2: The Sparus AUV frames

In this experiment, I establish the origin of the Sparus body to coincide with the model's center of gravity. The distance from the origin of F_b to the center of buoyancy is provided below.

$$\mathbf{r}^b_{cg} = \begin{bmatrix} 0 \\ 0 \\ 0 \end{bmatrix} \text{m}$$

$$\mathbf{r}^b_{bu} = \begin{bmatrix} 0 \\ 0 \\ -0.02 \end{bmatrix} \text{m}$$

3 The Dimension of Different Bodies of the Sparus AUV

To compute the dimensions of the different bodies, I followed the following steps:

- Split the Sparus prototype into 7 parts as shown in Table 1 and Figure 4 below.
- Measure the dimension of each part on the given figure using the **AutoCAD** software.
- Multiply the measurements taken by the ruler by the following scale factors to get the actual measurements:

The scale factor for the X-axis is given by:

$$X \text{ axis} = \frac{1600\,\text{mm}}{1703,93\,\text{mm}} = 0.9390$$

The scale factor for the Y-axis and Z-axis is given by:

$$Y \text{ axis}, Z \text{ axis} = \frac{230\,\text{mm}}{249,75\,\text{mm}} = 0.9390$$

Where: 1600 m and 230 m are the original length and diameter of the Sparus in millimeters

1703.93 mm and 249.75 mm are the measured equivalents of the length and diameter of the Sparus

Each part's respective dimensions are detailed in Figures 3,4 and 5 and Table 1 below.

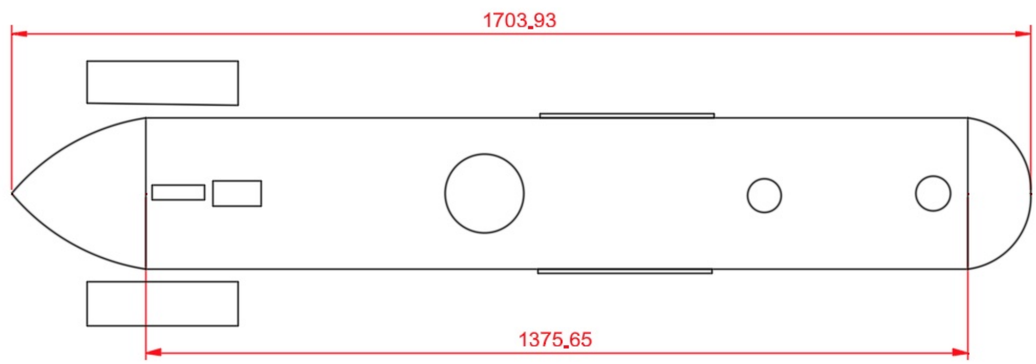

Figure 3: Top View Dimensions of the Sparus AUV

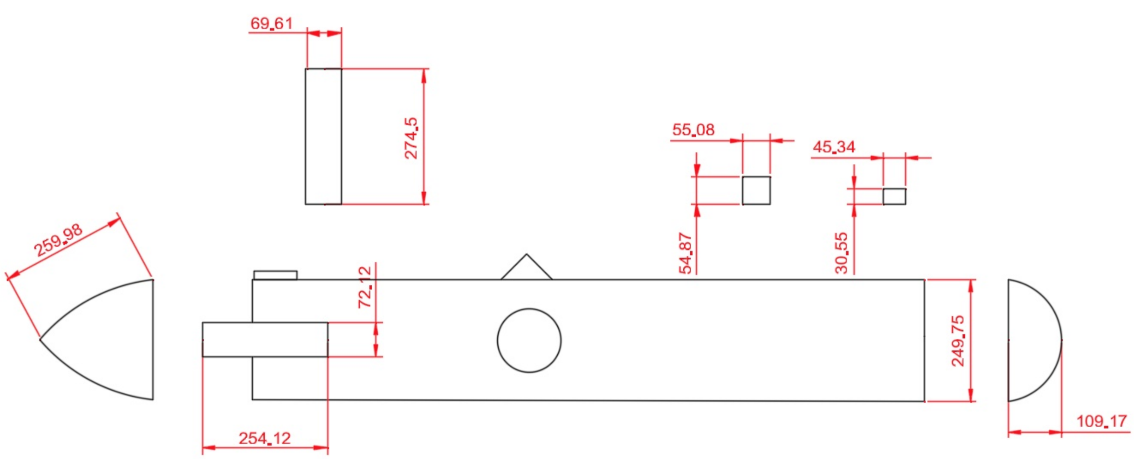

Figure 4: Side View Dimensions of the Sparus AUV

Part N0:	Part	Qty	Measured Value (mm)	Scaled Value (m)
1	Cylinder (Main Body)	1	**Length** = 1375.65 $\phi = 244.93$ $\phi = 244.93$	**Length** = 1.2925 $\phi = 0.2299$ $\phi = 0.2299$
2	Cone (Front Cover)	1	**Height** = 228.89 $\phi = 244.93$ $\phi = 244.93$	**Height** = 0.2149 $\phi = 0.2299$ $\phi = 0.2299$
3	Hemisphere (Rear Cover)	1	**Height** = 101.36 $\phi = 244.93$ $\phi = 244.93$	**Height** = 0.0952 $\phi = 0.2299$ $\phi = 0.2299$
4	Cuboid (Antenna)	1	**Length** = 69.61 **Width** = 23.80 **Height** = 274.5	**Length** = 0.06536 **Width** = 0.0223 **Height** = 0.2578
5	Side Thrusters	2	**Length** = 254.12 $\phi = 119.81$ $\phi = 119.81$	**Length** = 0.2386 $\phi = 0.1125$ $\phi = 0.1125$
6	Top Cylinders (DVL)	1	**Length** = 55.08 $\phi = 55.08$ $\phi = 54.87$	**Length** = 0.05 $\phi = 0.05$ $\phi = 0.05$
7	Top Cylinder (USBL)	1	**Length** = 45.34 $\phi = 45.34$ $\phi = 30.55$	**Length** = 0.04 $\phi = 0.04$ $\phi = 0.03$

Table 1: Saprus AUV Body Parts and their Dimensions

4 Analysis of Terms in the Global Real Mass Matrix for the Sparus AUV

Considering the given global real mass matrix explain all the terms: from which part the various terms in the matrix originate

The Global real mass matrix is given by:

$$M_{\substack{RB\\CO}} = \begin{bmatrix} 52 & 0 & 0 & 0 & -0.1 & 0 \\ 0 & 52 & 0 & 0.1 & 0 & -1.3 \\ 0 & 0 & 52 & 0 & 1.3 & 0 \\ 0 & 0.1 & 0 & 0.5 & 0 & 0 \\ -0.1 & 0 & 1.3 & 0 & 9.4 & 0 \\ 0 & -1.3 & 0 & 0 & 0 & 9.5 \end{bmatrix}$$

Let's break the matrix into four parts: M1, M2, M3 and M4 each representing a 3 x 3 matrix.

$$M_1 = \begin{bmatrix} 52 & 0 & 0 & \cdots & 0 & 0 \\ 0 & 52 & 0 & \cdots & 0 & 0 \\ 0 & 0 & 52 & \cdots & 0 & 0 \\ \vdots & \vdots & \vdots & \ddots & \vdots & \vdots \\ 0 & 0 & 0 & \cdots & 0 & 0 \\ 0 & 0 & 0 & \cdots & 0 & 0 \end{bmatrix}$$

The first 3x3 submatrix above provides information about the translational masses along the three main axes of the Sparus AUV. The values in the diagonal indicate the masses associated with linear motion in each respective direction. The fact that the values are the same across the diagonal suggests a symmetric mass distribution, at least in terms of translational masses. Here's the explanation for each term:

- 52 [a_{11}]: This represents the mass associated with the translational degree of freedom along the x-axis. It indicates how the Sparus II AUV responds to linear motion in the x-direction.
- 52 [a_{22}]: This represents the mass associated with the translational degree of freedom along the y-axis. Similarly, it indicates how the AUV responds to linear motion in the y-direction.
- 52 [a_{33}]: This represents the mass associated with the translational degree of freedom along the z-axis. It indicates how the AUV responds to linear motion in the z-direction.

$$M_2 = \begin{bmatrix} 0 & 0 & 0 & \cdots & 0 & 0 \\ 0 & 0 & 0 & \cdots & 0 & 0 \\ \vdots & \vdots & \vdots & \ddots & \vdots & \vdots \\ 0 & 0.1 & 0 & \cdots & 0 & 0 \\ -0.1 & 0 & 1.3 & \cdots & 0 & 0 \\ 0 & -1.3 & 0 & \cdots & 0 & 0 \end{bmatrix}$$

- 0.1 [a_{42}]: Coupling term betIen y-axis translation and z-axis rotation. $a_{42} = 0.1$, indicating a positive coupling effect. This suggests a positive coupling betIen linear motion along the y-axis and rotational motion about the z-axis.
- -0.1 [a_{51}]: Coupling term betIen x-axis translation and y-axis rotation. $a_{51} = -0.1$, indicating a negative coupling effect. This suggests a negative coupling betIen linear motion along the x-axis and rotational motion about the y-axis.
- 1.3 [a_{53}]: Coupling term betIen z-axis translation and y-axis rotation. $a_{53} = 1.3$, indicating a positive coupling effect. This suggests a positive coupling betIen linear motion along the z-axis and rotational motion about the y-axis.
- -1.3 [a_{62}]: Coupling term betIen y-axis translation and z-axis rotation. $a_{62} = -1.3$, indicating a negative coupling effect. This suggests a negative coupling betIen linear motion along the y-axis and rotational motion about the z-axis.

$$M_3 = \begin{bmatrix} 0 & 0 & 0 & \cdots & 0 & 0 \\ 0 & 0 & 0 & \cdots & 0 & 0 \\ \vdots & \vdots & \vdots & \ddots & \vdots & \vdots \\ 0 & 0 & \cdots & 0.5 & 0 & 0 \\ 0 & 0 & \cdots & 0 & 9.4 & 0 \\ 0 & 0 & \cdots & 0 & 0 & 9.5 \end{bmatrix}$$

- 0.5 [a_{44}]: Inertia term associated with rotational motion about the x-axis. $a_{44} = 0.5$, indicating the mass distribution and resistance to rotation about the x-axis.
- 9.4 [a_{55}]: Inertia term associated with rotational motion about the y-axis. $a_{55} = 9.4$, indicating the mass distribution and resistance to rotation about the y-axis.
- 9.5 [a_{66}]: Inertia term associated with rotational motion about the z-axis. $a_{66} = 9.5$, indicating the mass distribution and resistance to rotation about the z-axis.

$$M_4 = \begin{bmatrix} 0 & 0 & \cdots & 0 & -0.1 & 0 \\ 0 & 0 & \cdots & 0.1 & 0 & -1.3 \\ 0 & 0 & \cdots & 0 & 1.3 & 0 \\ \vdots & \vdots & \vdots & \ddots & \vdots & \vdots \\ 0 & 0 & 0 & \cdots & 0 & 0 \\ 0 & 0 & 0 & \cdots & 0 & 0 \end{bmatrix}$$

- -0.1 [a_{15}]: Coupling term betIen x-axis translation and z-axis rotation. $a_{15} = -0.1$, indicating a negative coupling effect. This suggests a negative coupling betIen linear motion along the x-axis and rotational motion about the z-axis.
- 0.1 [a_{24}]: Coupling term betIen y-axis translation and x-axis rotation. $a_{24} = 0.1$, indicating a positive coupling effect. This suggests a positive coupling betIen linear motion along the y-axis and rotational motion about the x-axis.
- -1.3 [a_{26}]: Coupling term betIen y-axis translation and z-axis rotation. $a_{26} = 0$, indicating no coupling. There's no contribution to the coupling betIen linear motion along the y-axis and rotational motion about the z-axis.
- 1.3 [a_{35}]: Coupling term betIen z-axis translation and y-axis rotation. $a_{35} = 1.3$, indicating a positive coupling effect. This suggests a positive coupling betIen linear motion along the z-axis and rotational motion about the y-axis.

4.1 Conclusion:

In conclusion, the analysis of the global real mass matrix for the Sparus AUV reveals crucial insights into the distribution of masses and coupling effects within the system. The matrix is decomposed into four parts, each representing specific dynamics: translational masses along the main axes, coupling effects between linear motion and rotational motion, and inertia terms for rotational motion about each axis. The values in the matrix provide a detailed understanding of how different components contribute to the overall dynamics of the Sparus AUV, essential for accurate modeling and control strategies in underwater robotics.

5 Analyzing the Order of Magnitude of the Rigid Body Real Mass Matrix

$$M_{\substack{RB\\CO}} = \begin{bmatrix} 52 & 0 & 0 & 0 & -0.1 & 0 \\ 0 & 52 & 0 & 0.1 & 0 & -1.3 \\ 0 & 0 & 52 & 0 & 1.3 & 0 \\ 0 & 0.1 & 0 & 0.5 & 0 & 0 \\ -0.1 & 0 & 1.3 & 0 & 9.4 & 0 \\ 0 & -1.3 & 0 & 0 & 0 & 9.5 \end{bmatrix}$$

Analysis:

In analyzing the real mass matrix, a compelling pattern of symmetry emerges in the relationship between the coupling terms. The elements a14, a15, a16, a24, a25, a26, a34, a35, a36, which describe the coupling between linear and rotational motions, exhibit a distinct screw-symmetric pattern when compared to their counterparts a41, a42, a43, a51, a52, a53, a61, a62, a63. This screw-symmetric behavior signifies that swapping the indices of these elements results in an equivalent coupling term with a reversed sign.

- **Diagonal Elements (Masses and Rotational Inertias):**
  - 52 (Linear Mass along x-axis):
    - A higher value indicates a larger mass along the x-axis.
    - It affects linear motion along the x-axis, influencing the Sparus's acceleration and deceleration in the forward and backward directions.
  - 52 (Linear Mass along y-axis):
    - Similar to the x-axis, a higher value indicates a larger mass along the y-axis.
    - It affects linear motion along the y-axis, influencing the Sparus's sideways acceleration and deceleration.
  - 52 (Linear Mass along z-axis):
    - A higher value indicates a larger mass along the z-axis.
    - It affects linear motion along the z-axis, influencing the Sparus's vertical acceleration and deceleration.
  - 0.5 (Rotational Inertia about x-axis):
    - This value represents the resistance to rotation (inertia) about the x-axis.
    - A higher value makes the Sparus more resistant to pitching motion (rotation about the x-axis).
  - 9.4 (Rotational Inertia about y-axis):
    - This value represents the resistance to rotation about the y-axis.
    - A higher value makes the Sparus more resistant to rolling motion (rotation about the y-axis).
  - 9.5 (Rotational Inertia about z-axis):

    * This value represents the resistance to rotation about the z-axis.
    * A higher value makes the Sparus more resistant to yawing motion (rotation about the z-axis).

- **Off-Diagonal Elements (Coupling Terms):**
  - **Coupling betIen y-axis Translation and x-axis Rotation (± 0.1):**
    * Positive coupling ($+0.1$): A motion along the y-axis introduces a rotation about the x-axis in the positive direction (pitching).
    * Negative coupling (-0.1): A motion along the y-axis introduces a rotation about the x-axis in the negative direction.
  - **Coupling betIen z-axis Translation and x-axis Rotation (± 1.3):**
    * Positive coupling ($+1.3$): A motion along the z-axis introduces a rotation about the x-axis in the positive direction (pitching).
    * Negative coupling (-1.3): A motion along the z-axis introduces a rotation about the x-axis in the negative direction.
  - **Coupling betIen x-axis Translation and y-axis Rotation (± 0.1):**
    * Positive coupling ($+0.1$): A motion along the x-axis introduces a rotation about the y-axis in the positive direction (rolling).
    * Negative coupling (-0.1): A motion along the x-axis introduces a rotation about the y-axis in the negative direction.
  - **Coupling betIen z-axis Translation and y-axis Rotation (± 1.3):**
    * Positive coupling ($+1.3$): A motion along the z-axis introduces a rotation about the y-axis in the positive direction (rolling).
    * Negative coupling (-1.3): A motion along the z-axis introduces a rotation about the y-axis in the negative direction.

Conclusions:

- **Diagonal Terms (Masses and Inertias):** The order of magnitude is around 10, indicating significant mass and rotational inertia.
- **Off-Diagonal Coupling Terms:** Coupling terms are smaller in magnitude compared to the diagonal terms, suggesting that the system's motion is mainly governed by its own masses and inertias.
- **Coupling Term Magnitudes:** Coupling term magnitudes involving rotational degrees of freedom are comparable, indicating similar strengths in the coupling effects.

6 Numerical Computation of Added Mass Matrices at the Buoyancy Center for Sparus AUV

To compute the added mass matrix at the boyancy center of the Sparus, I followed the following steps:

(a) Assume XY and ZX planes of symmetry. This reduces the added mass matrix coefficients expressed on the origin of the local frame of each body part of the Sparus AUV from 36 to 10 as shown below:

$$M_{\underset{CO}{RB}} = \begin{bmatrix} M_{a11} & 0 & 0 & 0 & 0 & 0 \\ 0 & M_{a22} & 0 & 0 & 0 & M_{a26} \\ 0 & 0 & M_{a33} & 0 & M_{a35} & 0 \\ 0 & 0 & 0 & M_{a44} & 0 & 0 \\ 0 & 0 & M_{a53} & 0 & M_{a55} & 0 \\ 0 & M_{a62} & 0 & 0 & 0 & M_{a66} \end{bmatrix}$$

(b) For simplicity, I split the body into 7 parts as follows:

- A Cone (rear cover)
- A Fin (part of the main body and the thrusters)
- A cylinder (the remaining part of the main body)
- An Hemisphere (front cover)
- A cuboid on top of the Sparus (Antenna)
- A cylinder (DVL)

These parts are therefore shown in figure 3 below:

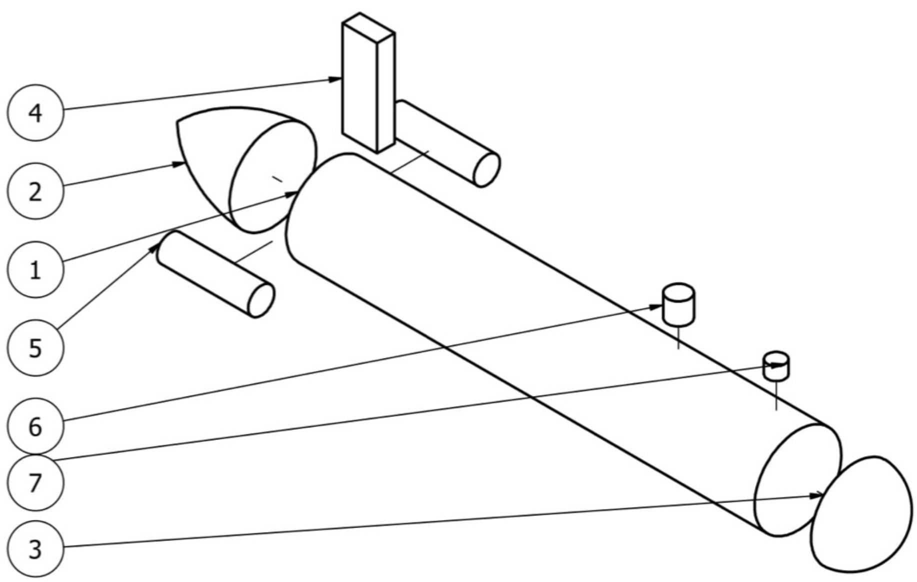

Figure 5: Exploded View Dimensions of the Sparus AUV

(c) Compute the added mass for each part using the following approaches:

i. Slender Body Theory: I used the slender body theory to approximate the added mass matrices for the cone (rear cover), the fin (part of the main body and the thrusters), the cylinder (remaining part of the main body), and the hemisphere (front cover).

However, since the slender body theory does not provide the M_{a11} coefficient, I used Lamb's K spherical approximation approach to approximate this value.

ii. Lamb's K Spherical Approximation: I used the spherical approximation approach to compute the added mass of the cuboid on top of the Sparus (i.e., antenna) and the M_{a11} coefficient for other parts that the slender body theory did not provide.

(d) Compute the distance from each gravity center of the body parts to the gravity center of the Sparus:

$$r_{\underset{b}{g}} = x\hat{\mathbf{i}} + y\hat{\mathbf{j}} + z\hat{\mathbf{k}}$$

where $\hat{\mathbf{i}}$, $\hat{\mathbf{j}}$, and $\hat{\mathbf{k}}$ are the unit vectors of the x, y, and z-axes, respectively.

(e) Derive the skew matrices for the distances between each body part's gravity center to the buoyancy center of the Sparus.

$$r_{\underset{b}{g}} = \begin{bmatrix} x \\ y \\ z \end{bmatrix}$$

$$\mathbf{S}(\mathbf{r}_{gb}) = \begin{bmatrix} 0 & -z & y \\ z & 0 & -x \\ -y & x & 0 \end{bmatrix}$$

(f) Derive the transformation matrices of each body part using the derived skew matrices:

$$\mathbf{H}(\mathbf{r}_{gb}) = \begin{bmatrix} \mathbf{I}_{3\times3} & \mathbf{S}^T(\mathbf{r}_{gb}) \\ \mathbf{0}_{3\times3} & \mathbf{I}_{3\times3} \end{bmatrix}$$

(g) Compute the added mass matrix of each body part at the buoyancy center of the Sparus using the mass matrix for each body part and their respective transformation matrix:

$$\mathbf{M}_{\text{CG}} = \mathbf{H}^T(\mathbf{r}_{\text{b}}) \cdot \mathbf{AM} \cdot \mathbf{H}(\mathbf{r}_{\text{b}})$$

(h) Compute the total added mass matrix at the buoyancy center of the Sparus by taking the sum of all the body parts' added mass matrices at the gravity center of the Sparus:

$$\mathbf{M}_{\text{Total}} = \sum \mathbf{M}_{\text{CG\_Part}}$$

The added mass matrix of the main body at the SPARUS center of gravity is:

$$M_{Mainbody} = \begin{bmatrix} 0.8549 & 0 & 0 & 0 & 0 & 0 \\ 0 & 56.4298 & 0 & 0 & 0 & 2.9472 \\ 0 & 0 & 56.4298 & 0 & -2.9472 & 0 \\ 0 & 0 & 0 & 0 & 0 & 0 \\ 0 & 0 & -2.9472 & 0 & 9.7188 & 0 \\ 0 & 2.9472 & 0 & 0 & 0 & 9.7188 \end{bmatrix}$$

The added mass matrices of the Antenna is:

$$M_{Antenna} = \begin{bmatrix} 0.4334 & 0 & 0 & 0 & 0 & 0 \\ 0 & 1.3870 & 0 & -0.0000 & 0 & 0 \\ 0 & 0 & 0 & 0 & 0 & 0 \\ 0 & -0.0000 & 0 & 0.0101 & 0 & 0 \\ 0 & 0 & 0 & 0 & 0.0020 & 0 \\ 0 & 0 & 0 & 0 & 0 & 0.0000 \end{bmatrix}$$

The added mass matrices of the Thruster 1 and 2 is:

$$M_{Thruster} = \begin{bmatrix} 0.1577 & 0 & 0 & 0 & 0 & 0 \\ 0 & 0 & 0 & 0 & 0 & 0.0000 \\ 0 & 0 & 1.8850 & 0 & -0.0000 & 0 \\ 0 & 0 & 0 & 0 & 0 & 0 \\ 0 & 0 & -0.0000 & 0 & 0.0090 & 0 \\ 0 & 0.0000 & 0 & 0 & 0 & 0.0090 \end{bmatrix}$$

The added mass matrices of other bodies (Antenna + Thruster 1 and 2, DVL and USBL) is:

$$M_{Other_bodies} = \begin{bmatrix} 0.7488 & 0 & 0 & 0 & 0 & 0 \\ 0 & 1.3870 & 0 & -0.0000 & 0 & 0.0000 \\ 0 & 0 & 3.7699 & 0 & -0.0000 & 0 \\ 0 & -0.0000 & 0 & 0.0101 & 0 & 0 \\ 0 & 0 & -0.0000 & 0 & 0.0201 & 0 \\ 0 & 0.0000 & 0 & 0 & 0 & 0.0181 \end{bmatrix}$$

The total added mass matrix of the Sparus at the center of Gravity is:

$$M_{\substack{RB \\ CG}} = \begin{bmatrix} 1.6037 & 0 & 0 & 0 & -0.1066 & 0 \\ 0 & 57.8168 & 0 & 0.3412 & 0 & 2.3993 \\ 0 & 0 & 60.1997 & 0 & -0.9416 & 0 \\ 0 & 0.3412 & 0 & 0.2082 & 0 & -0.1348 \\ -0.1066 & 0 & -0.9416 & 0 & 10.8321 & 0 \\ 0 & 2.3993 & 0 & -0.1348 & 0 & 9.9629 \end{bmatrix}$$

The total Added Mass Matrix after transforming it to the center of buoyancy is given by:

$$M_{\substack{RB \\ CB}} = \begin{bmatrix} 1.6037 & 0 & 0 & 0 & -0.3711 & 0.3390 \\ 0 & 57.8168 & 0 & 1.7042 & 0 & 2.3993 \\ 0 & 0 & 60.1997 & -2.0056 & -0.9416 & 0 \\ 0 & 1.7042 & -2.0056 & 1.3386 & -1.0670 & -0.1684 \\ -0.3711 & 0 & -0.9416 & -1.0670 & 10.9770 & -0.1637 \\ 0.3390 & 2.3993 & 0 & -0.1684 & -0.1637 & 10.1102 \end{bmatrix}$$

6.1 Conclusion:

- The added mass of the main body stands out as significantly larger in comparison to the other components, primarily due to its voluminous nature, resulting in the highest total inertial matrix.
- Examination of the global added mass matrix indicates that Sway and Heave navigation of the Sparus experience more pronounced added mass compared to Surge navigation. Similarly, the pitch and yaw rotations exhibit higher added mass. This observation aligns with the shape of the main body, suggesting it has greater ease in accelerating in the x-axis or rotating about it, necessitating more force for acceleration or rotation along other axes.
- The added masses of the sensors (Other bodies) are notably small, indicating a minimal impact on the overall system dynamics.

7 Comparing the added mass matrix at CG and CB

Total added mass matrix at the Sparus CG is given as follows:

$$M_{\substack{RB\\CG}} = \begin{bmatrix} 1.6037 & 0 & 0 & 0 & -0.1066 & 0 \\ 0 & 57.8168 & 0 & 0.3412 & 0 & 2.3993 \\ 0 & 0 & 60.1997 & 0 & -0.9416 & 0 \\ 0 & 0.3412 & 0 & 0.2082 & 0 & -0.1348 \\ -0.1066 & 0 & -0.9416 & 0 & 10.8321 & 0 \\ 0 & 2.3993 & 0 & -0.1348 & 0 & 9.9629 \end{bmatrix}$$

Transformed added mass matrix at the Sparus CB is given as follows:

$$M_{\substack{RB\\CB}} = \begin{bmatrix} 1.6037 & 0 & 0 & 0 & -0.3711 & 0.3390 \\ 0 & 57.8168 & 0 & 1.7042 & 0 & 2.3993 \\ 0 & 0 & 60.1997 & -2.0056 & -0.9416 & 0 \\ 0 & 1.7042 & -2.0056 & 1.3386 & -1.0670 & -0.1684 \\ -0.3711 & 0 & -0.9416 & -1.0670 & 10.9770 & -0.1637 \\ 0.3390 & 2.3993 & 0 & -0.1684 & -0.1637 & 10.1102 \end{bmatrix}$$

7.1 Conclusion:

- The transformed added mass matrix at the Sparus CB exhibits changes, particularly in off-diagonal elements, compared to the original added mass matrix at the Sparus CG.
- Off-diagonal elements, representing coupling effects between different degrees of freedom, also differ between the matrices. This implies that the relationship between different motion components is influenced by the specific locations of the center of gravity and center of buoyancy.
- The importance of considering the distance between the center of gravity and the center of buoyancy is underscored by the observed differences in matrix values. While the diagonal elements might be similar in this specific case, the variations in off-diagonal elements suggest

that the body's geometry and mass distribution are affected by the relative locations of these two points. Accounting for distance becomes crucial, especially when dealing with asymmetric body shapes or uneven mass distributions.

- In conclusion, both responses emphasize the significance of considering the distance between the center of gravity and the center of buoyancy when analyzing added mass matrices. The observed differences in matrix values highlight the impact of relative locations on added mass distribution and coupling effects, reinforcing the importance of this consideration in the analysis of underwater vehicles.

8 Comparing the Value of the Main Solid with Other Bodies

Added Mass Matrix of the Main Solid

$$M_{Mainbody} = \begin{bmatrix} 0.8549 & 0 & 0 & 0 & 0 & 0 \\ 0 & 56.4298 & 0 & 0 & 0 & 2.9472 \\ 0 & 0 & 56.4298 & 0 & -2.9472 & 0 \\ 0 & 0 & 0 & 0 & 0 & 0 \\ 0 & 0 & -2.9472 & 0 & 9.7188 & 0 \\ 0 & 2.9472 & 0 & 0 & 0 & 9.7188 \end{bmatrix}$$

Added Mass Matrix of Other Bodies

$$M_{Other_bodies} = \begin{bmatrix} 0.7488 & 0 & 0 & 0 & 0 & 0 \\ 0 & 1.3870 & 0 & -0.0000 & 0 & 0.0000 \\ 0 & 0 & 3.7699 & 0 & -0.0000 & 0 \\ 0 & -0.0000 & 0 & 0.0101 & 0 & 0 \\ 0 & 0 & -0.0000 & 0 & 0.0201 & 0 \\ 0 & 0.0000 & 0 & 0 & 0 & 0.0181 \end{bmatrix}$$

- **Magnitude Differences:**
  - The diagonal elements of $M_{\text{Main\_body}}$ exhibit larger values compared to those in $M_{\text{Other\_bodies}}$. For instance, the main solid has a significantly higher mass along the x, y, and z axes, indicating a greater influence on translational motion.
  - The off-diagonal elements in $M_{\text{Main\_body}}$ also have higher magnitudes, signifying stronger coupling effects between different degrees of freedom compared to $M_{\text{Other\_bodies}}$. This suggests that the main solid plays a more substantial role in influencing the dynamics of the Sparus AUV.
- **Distribution Patterns:**
  - $M_{\text{Main\_body}}$ exhibits a more complex distribution pattern with interconnected values, emphasizing the intricate coupling effects between translational and rotational motions of the main solid. In contrast, $M_{\text{Other\_bodies}}$ displays a simpler pattern, indicating comparatively weaker interactions.

8.1 Conclusion:

The higher values and more intricate distribution in $M_{\text{Main\_body}}$ underscore the significant contribution of the main solid to the added mass dynamics of the Sparus AUV. This suggests that the main solid has a more pronounced impact on the overall hydrodynamics and maneuverability of the AUV, emphasizing the need for precise modeling and consideration of its properties in simulations and control strategies.

9 Comparing the Value of the Added Mass and Real Mass Matrices

Real mass matrix:

$$M_{\underset{CO}{RB}} = \begin{bmatrix} 52.0000 & 0 & 0 & 0 & -0.1000 & 0 \\ 0 & 52.0000 & 0 & 0.1000 & 0 & -1.3000 \\ 0 & 0 & 52.0000 & 0 & 1.3000 & 0 \\ 0 & 0.1000 & 0 & 0.5000 & 0 & 0 \\ -0.1000 & 0 & 1.3000 & 0 & 9.4000 & 0 \\ 0 & -1.3000 & 0 & 0 & 0 & 9.5000 \end{bmatrix}$$

Added mass matrix at the Sparus CB is:

$$M_{\underset{CG}{RB}} = \begin{bmatrix} 1.6037 & 0 & 0 & 0 & -0.1066 & 0 \\ 0 & 57.8168 & 0 & 0.3412 & 0 & 2.3993 \\ 0 & 0 & 60.1997 & 0 & -0.9416 & 0 \\ 0 & 0.3412 & 0 & 0.2082 & 0 & -0.1348 \\ -0.1066 & 0 & -0.9416 & 0 & 10.8321 & 0 \\ 0 & 2.3993 & 0 & -0.1348 & 0 & 9.9629 \end{bmatrix}$$

The comparison between the real mass matrix ($M_{\underset{CO}{RB}}$) and the added mass matrix at the Sparus center of buoyancy ($M_{\underset{CB}{RB}}$) reveals differences in magnitude and distribution of values.

9.1 Comparing the Mass (M11):

$$M_{11}^{\binom{RB}{CO}} = 52.0000$$

$$M_{11}^{\binom{RB}{CB}} = 1.6037$$

The comparison between $M_{11}^{\binom{RB}{CO}}$ and $M_{11}^{\binom{RB}{CB}}$ shows a significant difference in magnitude, highlighting the disparity in mass contributions along the x-axis between the real mass matrix and the added mass matrix at the Sparus center of buoyancy which is due to the cone shape of the face of the AUV.

- **Magnitude Differences:**

– The two diagonal elements in (Sway and Heave motion) $M_{\underset{CB}{RB}}$ are slightly more compared to those in $M_{\underset{CO}{RB}}$, indicating that their is an added mass in the sway and heave motion due to the antenna and the side thrusters.

– Notably, the off-diagonal elements in $M_{\underset{CB}{RB}}$ are generally smaller, suggesting weaker coupling effects between different degrees of freedom compared to $M_{\underset{CO}{RB}}$.

9.2 Conclusion:

The differences in values between the real mass matrix and the added mass matrix at the Sparus center of buoyancy emphasize that the added mass at this point has a relatively smaller impact on the surge motion of the Sparus AUV. The maximum added mass value is experienced in the sway and heave motion and also during linear motion along the z-axis which causes a rotational motion about the y-axis due to the antenna.

10 Computing the Drag Matrices

To compute the drag matrices, I followed the following steps

(a) Assume XY and ZX planes of symmetry (the same symmetry assumption used to compute the added mass). This reduces the drag matrix coefficients expressed on the origin of the local frame of each body part of the Sparus robot from 36 to 10 as shown below

$$D_{NL} = \begin{bmatrix} K_{11} & 0 & 0 & 0 & 0 & 0 \\ 0 & K_{22} & 0 & 0 & 0 & K_{26} \\ 0 & 0 & K_{33} & 0 & K_{35} & 0 \\ 0 & 0 & 0 & K_{44} & 0 & 0 \\ 0 & 0 & K_{53} & 0 & K_{55} & 0 \\ 0 & K_{62} & 0 & 0 & 0 & K_{66} \end{bmatrix}$$

Split the Sparus model into 5 parts as follows:

- Front cover + Main body + Rear cover
- Thrusters
- Antenna
- DVL
- USBL

Figure 4: Exploded view of the Sparus Robot parts used to compute the drag matrices

(a) Compute the coefficients of the drag matrix for each part using the following expressions:
$K_{11} = \frac{1}{2} \cdot \rho \cdot S_x \cdot C_{D11}$ is the projected 3D drag coefficient in surge,

$K_{22} = \int_L \frac{1}{2} \cdot \rho \cdot C_{D22} \cdot D_y dx$ is the projected 2D drag coefficient in sway

$$K_{33} = \int_L \frac{1}{2} \cdot \rho \cdot C_{D33} \cdot D_z dx \quad \text{is the projected 2D drag coefficient in heave}$$
$$K_{44} = \int_L C_f(x) \cdot \frac{\rho V^2}{2} dxdy$$
$$K_{55} = \int_L x^2 \cdot K_3 3dx$$
$$K_{66} = \int_L x^2 \cdot K_{22} dx$$
$$K_{35} = K_{53} = \int_L x \cdot K_3 3dx$$
$$K_{26} = K_{62} = \int_L x \cdot K_{22} dx$$

The drag coefficients for each part are thus given as:

$$K_{\text{Main\_body}} = \begin{bmatrix} 1.9880 & 0 & 0 & 0 & 0 & 0 \\ 0 & 342.0000 & 0 & 0 & 0 & 0 \\ 0 & 0 & 342.0000 & 0 & 0 & 0 \\ 0 & 0 & 0 & 0 & 0 & 0 \\ 0 & 0 & 0 & 0 & 43.7760 & 0 \\ 0 & 0 & 0 & 0 & 0 & 43.7760 \end{bmatrix}$$

$$K_{\text{Antenna}} = \begin{bmatrix} 19.8188 & 0 & 0 & 0 & 0 & 0 \\ 0 & 32.7275 & 0 & 0 & 0 & 0 \\ 0 & 0 & 0 & 0 & 0 & 0 \\ 0 & 0 & 0 & 0 & 0 & 0 \\ 0 & 0 & 0 & 0 & 0 & 0 \\ 0 & 0 & 0 & 0 & 0 & 0 \end{bmatrix}$$

$$K_{(\text{thr1 and thr2})} = \begin{bmatrix} 3.5343 & 0 & 0 & 0 & 0 & 0 \\ 0 & 0 & 0 & 0 & 0 & 0 \\ 0 & 0 & 30.0000 & 0 & 0 & 0 \\ 0 & 0 & 0 & 0 & 0 & 0 \\ 0 & 0 & 0 & 0 & 0 & 0 \\ 0 & 0 & 0 & 0 & 0 & 0 \end{bmatrix}$$

$$K_{\text{DVL}} = \begin{bmatrix} 0.3003 & 0 & 0 & 0 & 0 & 0 \\ 0 & 1.8020 & 0 & 0 & 0 & 0 \\ 0 & 0 & 0 & 0 & 0 & 0 \\ 0 & 0 & 0 & 0 & 0 & 0 \\ 0 & 0 & 0 & 0 & 0 & 0 \\ 0 & 0 & 0 & 0 & 0 & 0 \end{bmatrix}$$

$$K_{\text{USBL}} = \begin{bmatrix} 0.7928 & 0 & 0 & 0 & 0 & 0 \\ 0 & 2.6915 & 0 & 0 & 0 & 0 \\ 0 & 0 & 0 & 0 & 0 & 0 \\ 0 & 0 & 0 & 0 & 0 & 0 \\ 0 & 0 & 0 & 0 & 0 & 0 \\ 0 & 0 & 0 & 0 & 0 & 0 \end{bmatrix}$$

$$K_{\text{Total}} = \begin{bmatrix} 26.4342 & 0 & 0 & 0 & 0 & 0 \\ 0 & 379.2210 & 0 & 0 & 0 & 0 \\ 0 & 0 & 372.0000 & 0 & 0 & 0 \\ 0 & 0 & 0 & 0 & 0 & 0 \\ 0 & 0 & 0 & 0 & 43.7760 & 0 \\ 0 & 0 & 0 & 0 & 0 & 43.7760 \end{bmatrix}$$

Some Key Observations:

- On surge, the antenna and the thrusters are subjected to the largest drag forces.
- The main body is subjected to a small drag force on surge. On the other hand, it is subjected to a large drag force in sway and heave. This can be attributed to its streamlined-like shape. The robot can easily move in water in surge, but requires extra force in sway and heave because its surface area is significantly larger and a rectangular-like shape does not seem to be of help unlike the front cover which is hemisphere.
- Similarly, the drag matrix of the sensors (USBL and DVL) reveals that they would be exposed to only significantly small drag force and would have little to no effect compared to drag effect of the main body.

10.1 Conclusion:

For the main body drag coefficient, movement in the y and z direction will create a much bigger friction force due to the big difference in the projected surface area. Minor parts such as DVL and USBL contribute a relatively low contribution to the friction forces and moment. However, it is a different case for the antenna. Because of the height of this component, it contributes a rather significant friction force and a small amount of turning moment, it is important to consider including the antenna for the modelization process.

11 Validating the Simulator

To complete the simulator, I first derived all the dynamic equation parameters required to complete the simulator. After this I ran a few experiments to validate our model.

11.1 Derive the dynamic equation parameters

(a) Derive the global mass matrix by taking the sum of the total rigid-body mass matrix $\left(M_B^b\right)$ and the total added mass matrix $\left(M_A^b\right)$

$$M_G^b = M_B^b + M_A^b$$

NB: since both matrices represent the mass matrix at Sparus CG, there is no need to transform them

$$M_{\substack{RB\\CO}} = \begin{bmatrix} 52.0000 & 0 & 0 & 0 & -0.1000 & 0 \\ 0 & 52.0000 & 0 & 0.1000 & 0 & -1.3000 \\ 0 & 0 & 52.0000 & 0 & 1.3000 & 0 \\ 0 & 0.1000 & 0 & 0.5000 & 0 & 0 \\ -0.1000 & 0 & 1.3000 & 0 & 9.4000 & 0 \\ 0 & -1.3000 & 0 & 0 & 0 & 9.5000 \end{bmatrix}$$

(a) Derive the Coriolis-centripetal matrix as follows:

$$C(v) = \begin{bmatrix} 0_{3\times3} & -S\left(M_{11}v_1 + M_{12}v_2\right. \\ -S\left(M_{11}v_1 + M_{12}v_2\right. & -S\left(M_{21}v_1 + M_{22}v_2\right. \end{bmatrix}$$

where:

v_1 and v_2 are the linear and angular speed vectors along the x, y and z axes respectively and M is the 6×6 system inertia matrix and they are expressed as follows

$$M_G^b = \begin{bmatrix} M_{11} & M_{12} \\ M_{21} & M_{22} \end{bmatrix}; \quad v_1 = \begin{bmatrix} u \\ v \\ w \end{bmatrix}; \quad v_2 = \begin{bmatrix} p \\ q \\ r \end{bmatrix}$$

(a) Derive the sum of all the body drag forces

To apply the drag matrices $\left(K_q^{bi}\right)$ I have computed for each body, I folloId the steps below

(a) Compute the speed at the Buoyancy center of each body from the DVL position as follows

$$V_{b_i/n}^b = H\left(\overrightarrow{C_{DVL}b_i}\right) V_{C_{DVL}/n}^b$$

where $V_{b_i/n}^b$ is the velocity at the buoyancy center of body i, $H\left(\overrightarrow{C_{DVL}b_i}\right)$ is the homogeneous transformation matrix from the DVL to the body, and $V_{C_{DVL}/n}^b$ is the velocity of the submarine at DVL (b) Compute the drag force on the body expressed at its buoyancy center b_i as follows

$$\tau_{b_i,i}^b = K_{q,i}^{bi} \cdot \left|V_{b_i/n}^b\right| \cdot V_{b_i/n}^b$$

(c) Move each global drag force from the body parts' center to the gravity center of the Sparus submarine

$$\tau_{g_0,i}^b = H^T\left(\overrightarrow{g_0 b_i}\right) \cdot \tau_{b_i,i}^b$$

where $\tau_{b_i,i}^{b}$ is the drag force matrix of a part at its buoyancy center, $H^T\left(\overrightarrow{g_0 b_i}\right)$ is the homogeneous transform matrix derived from the distance betIen the part buoyancy center and Sparus gravity center, and $\tau_{g_0,i}^{b}$ is the drag force matrix of a part at the sparus gravity center,

(d) Take the sum of all the drag forces at the gravity center

$$\tau^{g_0} = \tau_0^{g_0} + \sum \tau_i^{g_0}$$

where $\tau_0^{g_0}$ is the drag force on the main body, $\tau_i^{g_0}$ are the drag matrices of other parts, and τ^{g_0} is the global drag matrix for the submarine.

(a) Map the thrusters based on their locations.

Given the thruster force vector

$$F_T^b = \begin{bmatrix} F_{T1}^b \\ F_{T2}^b \\ F_{T3}^b \end{bmatrix}$$

and thruster position vector

$$r = \begin{bmatrix} r_{T1}^b \\ r_{T2}^b \\ r_{T3}^b \end{bmatrix}$$

The thruster forces and moments and moments can be represented by

$$U^b = E^b \cdot F_T^b$$

where:

U^b represents the force and moment vectors at the sparus origin, E^b depicts the matrix describing the positions of the thrusters (given in the homework), and F^b represents a vector of the forces produced by thrusters 1,2 , and 3 respectively.

The above expression can be further simplified as follows

$$\Longrightarrow U^b = \begin{bmatrix} F_x \\ F_y \\ F_z \\ M_x \\ M_y \\ M_z \end{bmatrix} = \begin{bmatrix} 0 & 1 & 1 \\ 0 & 0 & 0 \\ 1 & 0 & 0 \\ 0 & 0 & 0 \\ 0 & 0 & 0 \\ 0 & -0.17 & 0.17 \end{bmatrix} \cdot \begin{bmatrix} F_{T1}^b \\ F_{T2}^b \\ F_{T3}^b \end{bmatrix}$$

11.2 Validating the Model

After deriving the dynamic equation parameters, I completed the simulator with the derived parameters and ran a few experiments to validate our model by manipulating the power applied to the 3 thrusters namely vertical, left and right thruster as indicated below

11.3 Experiment 1: All Three Thrusters Off

To visualize the effect of the drag forces on the submarine, I turned off all the thruster power and observed the ROV's behaviour.

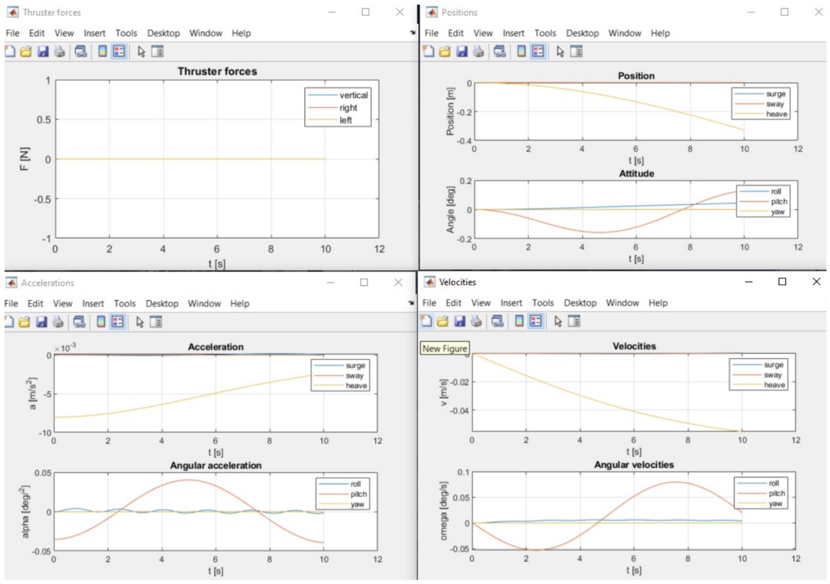

Figure 6: Model Behaviour with all Thrusters OFF.

From the diagram above, I can see that no thrust forces do not stop the submarine from changing position. However, both the linear and the angular velocity and acceleration charts reveal that this motion however is random and fails to converge to an equilibrium. This is since there was no external force to control the drag and other dissipative forces.

11.4 Experiment 2: only vertical thruster ON

This validation experiment aims to obtain a downward movement in the z-direction (heave). Therefore, I turned off both the left and right thrusters, but powered the vertical thruster to 20%. As expected, the submarine clearly shows heave movement in the position charts shown in Figure 6 below.

Powering only the vertical thrusters hover causes instability in the angular accelerations as the robot rotates randomly about the 3 axes. This signifies that the side thrusters would also perform a significant role in stabilizing the vehicle.

11.5 Experiment 3: Left and Right thrusters ON

This validation experiment aims to obtain a forward movement. Therefore, I set both the left and right thruster power to 20% and the vertical thruster to 0%. Similarly, as expected, the ROV clearly shows surge movement in the below charts.

Similar to experiment 2, powering only the side thrusters also causes instability in the angular accelerations as the robot rotates randomly about the 3 axes. This also signifies that the vertical thrusters would also perform a significant role in stabilizing the vehicle.

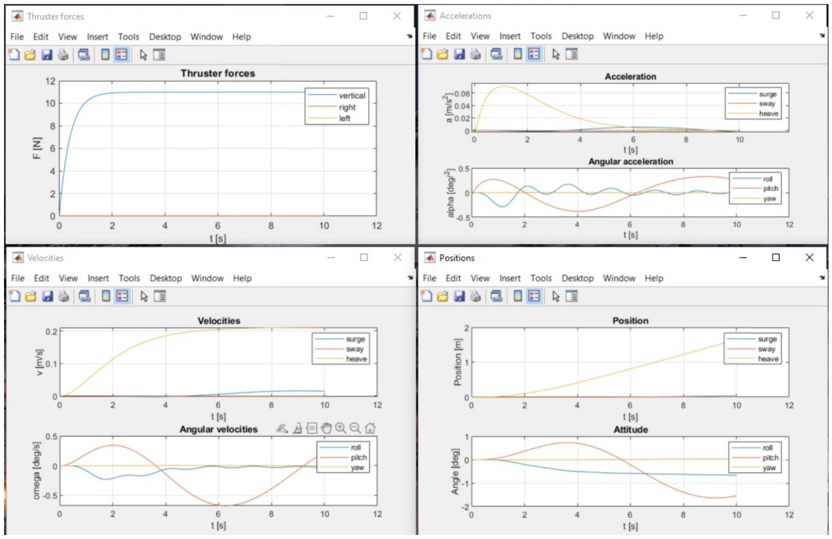

Figure 7: Model Behaviour with only vertical Thruster.

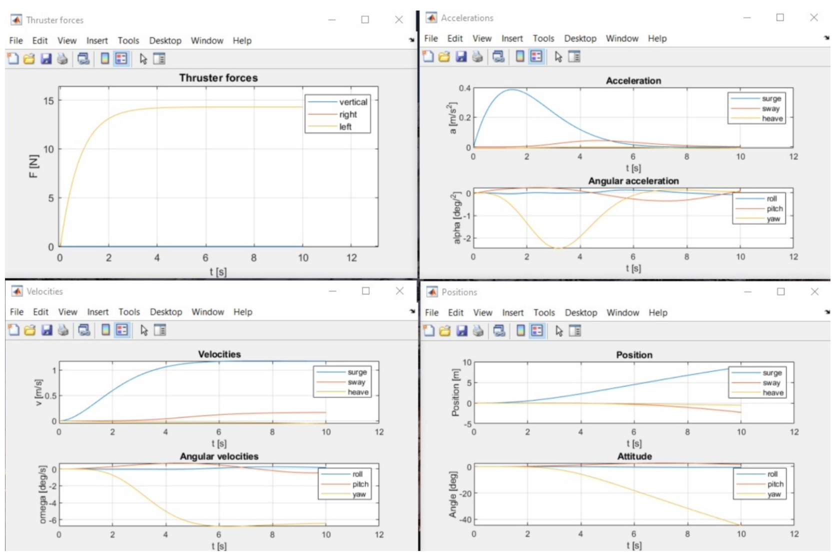

Figure 8: Model Behaviour with Left and Right Thrusters ON.

11.6 Experiment 4: All thrusters powered

This experiment aims to visualize how the Sparus model would behave if all the thrusters were powered. The corresponding output is shown in Figure 8 below

The position charts reveal that the ROV attained positions between 0 to 10 meters over 10s while trying to stabilize itself. This can also be seen from the plot representing Altitude Angle. Also, the yaw angle seems to increase sufficiently with the increase in position as compared to roll and pitch angles because the AUV is trying to find stability.

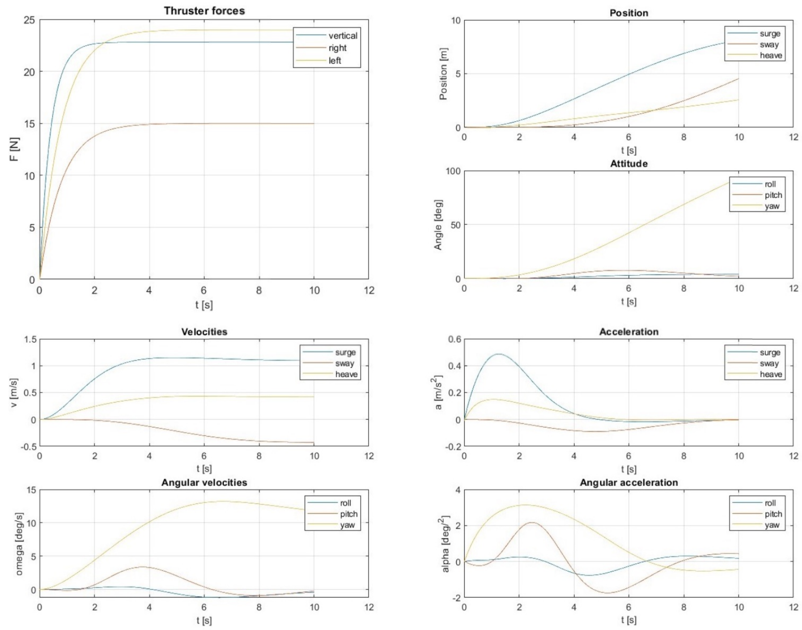

Figure 9: Model Behaviour with all Thursters ON

12 Analyzing the Impact of Coefficients on Global Mass Matrix through Simulation under Imposed Linear Acceleration.

Experiment: Exploring the influence of rigid-body part matrices on Sparus' global mass matrix, I compared the dynamics of the complete Sparus with an incomplete version. I conducted a baseline experiment using the original global mass matrix. Subsequently, a part was removed from the submarine to decrease the global mass matrix. I simulate the model in x (surge), y (heave), and z (yaw) directions, facilitating a comprehensive comparison of the two models' performance. Employing a 3% threshold for comparison alloId for the safe removal of bodies contributing to a relative modeling error of 3% or loIr.

12.1 Case 1: Motion along X-direction (Surge)

For this experiment, I set the power of the side thrusters to 20% while I kept the vertical thruster at 0% power. The results of our simulation over a duration of 40 s is shown the figure below:

From the test above, I can see that taking out the DVL causes the least amount of error, especially in surge motion.

12.2 Case 2: Motion along Y-direction (Sway)

The results of the simulation over a duration of 40 s is shown in the figure below.

From the above test, no body shows relative error less than 5

Thrusters - in forward direction with 20% Power each, Duration of Simulation: 40 sec.			
Case	Motion	Measurements	% Relative Error
No Body Removed	Heave(m):	-16.98	-
	Pitch(deg):	32	
	Surge(m):	37	
DVL (Removed)	Heave(m):	-17	0.117
	Pitch(deg):	31.957	0.134
	Surge(m):	36	2.703
Antenna (Removed)	Heave(m):	-5.5	67.61
	Pitch(deg):	8	75
	Surge(m):	62	67.57
USBL (Removed)	Heave(m):	-14	17.55
	Pitch(deg):	31	3.125
	Surge(m):	34	8.11
Thrusters (Removed)	Heave(m):	-21	23.67
	Pitch(deg):	44	37.5
	Surge(m):	33	10.81

Figure 10: Impact of the surge motion on different coefficients in the global mass matrix.

Thrusters- in downward direction with 20% power each, Duration of Simulation: 40 sec.			
No Body Removed	Heave(m):	9	% Relative Error
	Pitch(deg):	-14	
	Surge(m):	-1.2	
DVL (Removed)	Heave(m):	8	11.111
	Pitch(deg):	-14	0.0
	Surge(m):	-1.0	16.67
Antenna (Removed)	Heave(m):	9	0.0
	Pitch(deg):	-16.45	17.5
	Surge(m):	-0.6	50.0
USBL (Removed)	Heave(m):	8	11.111
	Pitch(deg):	-16	14.28
	Surge(m):	-0.8	33.33
Thrusters (Removed)	Heave(m):	14	55.55
	Pitch(deg):	-2	85.7
	Surge(m):	0.87	8

Figure 11: Impact of the sway motion on different coefficients in the global mass matrix.

12.3 Case 3: Motion along Z-direction (Heave)

For this experiment, I set the power of the left and vertical thrusters to 0%, but the right thruster to 20% to create a counterclockwise rotation about the z-axis (yaw). The results of our simulation over a duration of 40 s are shown in the figure below.

From the above test, it can be observed that removing the DVL and USBL has the least effect on the motion.

12.4 Conclusion

Based on the conducted experiments, I recommend excluding the DVL and USBL components specifically during surge and yaw motions. While removing these parts may not adversely affect the dynamic performance of our Sparus, it is crucial to retain all components to ensure balance, as these parts have been considered in our dynamic equations.

Thrusters- in downward direction with 20% power each, Duration of Simulation: 40 sec.			
No Body Removed	Heave(m):	9	% Relative Error
	Pitch(deg):	-14	
	Surge(m):	-1.2	
DVL (Removed)	Heave(m):	8	11.111
	Pitch(deg):	-14	0.0
	Surge(m):	-1.0	16.67
Antenna (Removed)	Heave(m):	9	0.0
	Pitch(deg):	-16.45	17.5
	Surge(m):	-0.6	50.0
USBL (Removed)	Heave(m):	8	11.111
	Pitch(deg):	-16	14.28
	Surge(m):	-0.8	33.33
Thrusters (Removed)	Heave(m):	14	55.55
	Pitch(deg):	-2	85.7
	Surge(m):	0.87	8

Figure 12: Impact of the yaw motion on different coefficients in the global mass matrix.

13 Simulating the Influence of Drag Forces by Evaluating the Effects Under Constant Linear Speed.

To evaluate the influence of drag forces on Sparus dynamics, thruster powers were uniformly set to 20% in all experiments to ensure a constant linear speed. The Sparus dynamic model was then simulated by removing the drag matrix, and the model's response was compared with and without the drag matrix.

The outcomes of this experiment are shown in Figure 9.

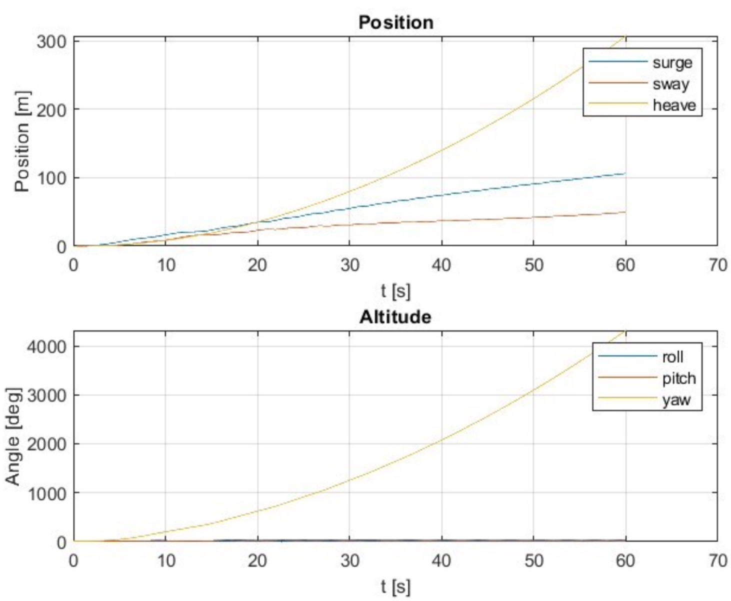

Figure 13: Model Behaviour with Zero Drag Force.

From the figure above, I can infer that in the absence of drag, the AUV covers more distance as the opposing forces are decreased.

13.1 Conclusion

In conclusion, the simulations conducted to investigate the influence of drag forces on different bodies, with a focus on maintaining a constant linear speed by setting thruster powers to 20%, yielded valuable insights. Removing the drag matrix from the Sparus dynamic model showcased a notable effect on the AUV's performance. Specifically, the increased distance covered in the absence of drag highlights the significant impact of drag forces on the overall dynamics of the system. These findings emphasize the importance of accounting for drag forces in underwater vehicle design and simulation to enhance predictive accuracy and inform optimization strategies.

14 CODE GUIDE

These are the list of files and folders added to the report and a description of what they mean:

- `Sparus_Calibration.dwg`: AutoCAD file of the dimensions.
- `Added Mass and Drag.m`: Added Mass and Drag Matrices Calculation.
- `Parameter.m`: Parameter file.
- `RovModel.m`: RovModel File.

References

- Robots marins et sous-marins Perception, modélisation, commanded, September 2014, DOI: 10.51257/a-v1-s7783
- Fossen, Thor I. (Apr. 2011). Handbook of Marine Craft Hydrodynamics and Motion Control. John Wiley and Sons. ISBN: 9781119991496. DOI: 10.1002/9781119994138.
- IQUA-Robotics (2022). Sparus II AUV. URL: https://iquarobotics.com/sparus-ii-auv